(38) J. W. Buchler in "Porphyrins and Metalloporphyrins", K. M. Smith, Ed., American Elsevier, New York, N.Y., 1975, pp 157–244.
(39) R. D. Shannon and C. T. Prewitt, Acta Crystallogr., Sect. B, 25, 925 (1969).
(40) J. L. Hoard in ref 38, Chapter 8.
(41) B. Morosin and A. Narath, J. Chem. Phys., 40, 1958 (1966). A Cr(Cl) bond length of about 2.34 Å is typical for six-coordinate Cr(III) complexes. See

also R. Stromberg and I. Larkin, Acta Chem. Scand., 23, 343 (1969).
(42) Abbreviations: TPP, dianion of meso-tetraphenylporphin; OEP, dianion of octaethylporphyrin; py, pyridine; DMF, N,N-dimethylformamide; THF, tetrahydrofuran; 1-MeIm, 1-methylimidazole; Me₂SO, dimethyl sulfoxide; THTP, tetrahydrothiophene; sec-BuNH₂, sec-butylamine; 3,4-Lut, 3,4-lutidine (3,4-dimethylpyridine); 3,5-Lut, 3,5-lutidine; 4-CN-py, 4-cyanopyridine; Pip, piperidine.

Structural Evidence for Xenon–Chlorine Bonding: Neutron and X-Ray Diffraction Determinations of the Structure of Cesium and Rubidium Trioxodichloroxenate(VI) Chloride, $Cs_9(XeO_3Cl_2)_4Cl$ and $Rb_9(XeO_3Cl_2)_4Cl^1$

R. D. Willett,* S. W. Peterson, and B. A. Coyle

Contribution from the Chemistry Division, Argonne National Laboratory, Argonne, Illinois 60439. Received January 5, 1977

Abstract: The compounds $XeO_3 \cdot 2.25CsCl$ and $XeO_3 \cdot 2.25RbCl$ have been structurally characterized as cesium and rubidium trioxodichloroxenate(VI) chloride, $M_9(XeO_3Cl_2)_4Cl$, using single-crystal counter diffraction methods. The crystals are body-centered tetragonal, point group $4/m$, with $a = 16.56$ Å and $c = 7.10$ Å for the Cs salt and $a = 15.97$ Å and $c = 6.91$ Å for the Rb salt, and contain eight $XeO_3 \cdot 2.25MCl$ formula units per unit cell. The structures have been refined in the space group $I\bar{4}$ to R factors of 8.3% for the Cs compound using neutron data and 10.4% for the Rb compound using x-ray data. The crystal structures contain infinite chains, parallel to c, of XeO_3Cl^- units linked by nearly linear chlorine bridges. The metal cations and one-ninth of the chlorine atoms are separated from the repeating polymeric unit $XeO_3Cl_2^{2-}$ by nonbonding distances. The xenon coordination is octahedral (distorted) with three terminal oxygen neighbors (in the Cs salt) at 1.77 Å, one terminal Cl neighbor at 2.96 Å, and two bridging Cl neighbors at 2.95 and 2.97 Å.

We wish to report the first conclusive demonstration of the existence of stable Xe–Cl bonding at normal temperatures. Stable chemical compounds of xenon with the strongly electronegative elements fluorine and oxygen are well known. Since chlorine is nearly as electronegative as oxygen, it is to be expected that Xe–Cl bonds may exist. Perlow and Perlow[2] have shown through Mossbauer studies that $XeCl_2$ and $XeBr_2$ are formed at 4 K by the radioactive decay of the corresponding iodine compounds. Attempts to synthesize $XeCl_2$ or $XeCl_4$ by chemical means have not been successful, but recently $RbCl$ and $CsCl$ salts of XeO_3 have been isolated.[3] Although they are of different stoichiometry from the potassium fluoride salt of XeO_3, $K(XeO_3)F$,[4] these chloride salts might also be expected to contain halogen bridges.

Indeed, LaBonville, Ferraro, and Spittler,[3] although they formulated them as $XeO_3 \cdot 2MCl$, have observed vibrational transitions in the far IR for these compounds which they assigned as Xe–Cl stretching modes. Thus in order to shed further light on the existence of Xe–Cl bonds at ambient temperature, we have solved the crystal structures and found the specimens selected to have the stoichiometry $XeO_3 \cdot 2.25MCl$ and to be structurally $M_9(XeO_3Cl_2)_4Cl$.

Structure Determination

Samples of both a rubidium and a cesium chloride addition compound with XeO_3, prepared by reacting $RbCl$ and $CsCl$ in a 2:1 ratio with XeO_3,[3] were studied. The crystals selected were well-shaped tetragonal prisms with $a = 16.56$ and $c =$

* ACEA Faculty Research Participant, 1972–1973. Department of Chemistry, Washington State University, Pullman, Wash. 99164.

7.10 Å for Cs and $a = 15.97$ and $c = 6.91$ Å for Rb. The crystal densities were greater than that of methylene iodide (3.32 g cm⁻³), hence not measured; $\rho_{calcd} = 3.40$ and 3.81 for Rb and Cs, respectively, on the assumption that $Z = 8$. Precession photographs established the systematic extinctions to be $h + k + l = 2n + 1$ and the possible space groups $I4/m$ and $I\bar{4}$ for both compounds.

It was subsequently discovered that smaller amounts of a second phase existed in both Rb and Cs samples. These were identified by X-ray photography as triclinic phases with cell parameters $a = 10.10$, $b = 12.77$, $c = 10.00$ Å $\alpha = 91.30$, $\beta = 92.22$, and $\gamma = 100.64°$ for the Rb compound. The density of the second Rb phase was less than 3.32 and was measured as 3.19 g cm⁻³. This value leads to possible stoichiometries of $(RbCl)_{1.87} \cdot XeO_3$ or $RbCl \cdot XeO_3$ for assumed $Z = 6$ and 8, respectively, for the triclinic phase. All further structural work was concentrated on the tetragonal phase. The above findings, however, cast doubt on the initial assumed stoichiometry of $(RbCl)_2 \cdot XeO_3$ for the tetragonal phase.

Since both salts exhibited very severe decomposition upon exposure to the x-ray beam, peak-height data were collected using an automated GE diffractometer. A total of 1095 reflections were collected for the Cs salt and 1102 for the Rb salt. In each case, it was necessary to use three crystals in order to complete the data collection. The distribution of intensities was indicative of an acentric structure.[5]

The main heavy atom (Xe, 2M) positions, indicated by the formula $XeO_3 \cdot 2MCl$, were readily located using both the Patterson function and direct methods. However, extra peaks found in high symmetry positions on subsequent Fourier maps were eventually attributed to extra M⁺ and Cl⁻ ions requiring a reformulation of the stoichiometry to $XeO_3 \cdot 2.25MCl$. In-

Table I. Final Positional, Thermal, and Site Occupancy Parameters[a,b] for $Cs_9(XeO_3Cl_2)_4Cl$ (Neutron Data) and $Rb_9(XeO_3Cl_2)_4Cl$ (X-Ray Data)

	f^c	a^c	x	y	z	β_{11}	β_{22}	β_{33}	β_{12}	β_{13}	β_{23}
Cs(1)	0.558	0.98 (2)	0.1015 (3)	0.3747 (3)	0.0091 (15)	37 (2)	39 (2)	129 (16)	5 (2)	−6 (8)	−9 (8)
Rb(1)		0.99 (4)	0.0985 (30)	0.3761 (30)	0.0109 (10)	42 (2)	46 (3)	189 (15)	6 (2)	−10 (5)	−12 (5)
Cs(2)	0.558	0.98 (2)	0.4168 (3)	0.3150 (3)	0.0213 (14)	29 (2)	23 (2)	249 (19)	−6 (2)	−3 (7)	0 (6)
Rb(2)		1.00 (4)	0.4178 (3)	0.3156 (3)	0.0383 (10)	45 (2)	27 (2)	330 (18)	−5 (2)	−6 (6)	17 (5)
Cs(0)	0.558	0.247 (8)	0	0	0	38 (8)	38	122 (26)	0	0	0
Rb(0)		0.253 (13)		0	0	80 (10)	80	200 (38)	0	0	0
			0								
Xe	0.48	0.80 (2)	0.2320 (4)	0.1092 (4)	−0.0182 (18)	23 (2)	25 (3)	130 (22)	−9 (2)	−8 (8)	−11 (9)
		0.70 (3)	0.2330 (2)	0.1051 (2)	−0.0345 (7)	22 (2)	26 (2)	203 (13)	−5 (1)	1 (4)	−20 (4)
Cl(0)	0.598	0.247	0.5	0.5	0	22 (2)	22	175 (12)	0	0	0
		0.253	0.5	0.5	0	19 (10)	19	124 (57)	0	0	0
Cl(1)	0.958	1.01 (1)	0.4103 (1)	0.1074 (1)	0.0043 (10)	28 (1)	28 (1)	199 (8)	0 (1)	8 (5)	7 (5)
		0.98 (5)	0.4152 (6)	0.1087 (6)	0.011 (2)	28 (5)	26 (5)	224 (40)	2 (3)	4 (13)	32 (11)
Cl(2)	0.958	0.80	0.2479 (6)	0.2386 (6)	0.2659 (13)	45 (3)	44 (3)	137 (19)	3 (2)	−5 (5)	−25 (6)
		0.70	0.2437 (13)	0.2301 (9)	0.282 (3)	56 (9)	23 (8)	191 (50)	−14 (7)	47 (18)	−61 (16)
O(1)	0.575	0.80	0.1278 (4)	0.1311 (5)	−0.031 (3)	18 (2)	68 (4)	429 (41)	−9 (3)	2 (10)	−21 (16)
		0.70	0.123 (2)	0.122 (2)	−0.058 (5)	1.4 (6)[d]					
O(2)	0.575	0.80	0.2337 (11)	0.0347 (7)	0.160 (2)	77 (7)	22 (4)	377 (40)	−3 (4)	46 (12)	33 (9)
		0.70	0.241 (5)	0.022 (5)	0.113 (12)	6.7 (18)[d]					
O(3)	0.575	0.80	0.2408 (10)	0.0490 (10)	−0.226 (2)	52 (7)	60 (7)	312 (34)	−7 (6)	−15 (14)	−85 (13)
		0.70	0.246 (5)	0.059 (5)	−0.231 (13)	7.9 (19)[d]					
Xe*	0.48	0.20	0.234 (2)	0.149 (2)	0.097 (5)	10 (10)	50 (16)	175 (84)	7 (10)	−35 (23)	53 (34)
		0.30	0.2390 (6)	0.1495 (6)	0.0986 (14)	34 (4)[d]	30 (4)	158 (23)	6 (3)	−4 (8)	23 (9)
Cl(2)*	0.958	0.20	0.208 (2)	0.050 (2)	−0.208 (5)	4.1 (8)[d]					
		0.30	0.216 (5)	0.051 (5)	−0.243 (12)	7.0 (14)[d]					
O(1)*	0.575	0.20	0.127 (2)	0.175 (2)	0.075 (5)	41 (15)	76 (16)	96 (57)	38 (13)	19 (22)	−15 (27)
		0.30	0.130 (5)	0.160 (5)	0.136 (12)	1.8 (14)[d]					
O(2)*	0.575	0.20	0.232 (2)	0.067 (3)	0.242 (8)	11 (11)	67 (20)	280 (112)	−6 (14)	−11 (34)	96 (42)
		0.30	0.218 (7)	0.037 (6)	0.201 (17)	3.8 (19)[d]					
O(3)*[e]	0.575	0.20	0.239 (3)	0.252 (3)	0.221 (7)	0.3 (8)[d]					

[a] Uncertainties listed in parentheses. [b] The anisotropic thermal parameters are defined by $T = \exp[-(\beta_{11}h^2 + \cdots + 2\beta_{12}hk + \cdots)]$; values reported are multiplied by 10^4. [c] The symbol f denotes neutron scattering amplitudes from G. E. Bacon, *Acta Crystallogr., Sect. A*, **28**, 357 (1972), and the symbol a denotes the occupancy factor for each site. [d] Isotropic temperature factor. [e] O(3)* could not be located from the x-ray data.

clusion of the additional scattering matter improved the R factor and permitted further refinement. However, the light atom positions were highly uncertain. Difference Fouriers displayed confusing weaker maxima which were eventually traced to a structural disorder resulting from the existence of two rather equivalent sites for XeO_3Cl^- groups. Further refinement, including Xe fractional site occupancy, proceeded best in the acentric space group $I\bar{4}$. In the Cs salt about 80% of Xe atoms were found in site 1 and 20% in site 2 while the comparable figures for the Rb salt were about 70 and 30%. The nature of the disorder made it impossible, from the x-ray data, to locate the light atoms accurately or even to ascertain that the species at site 2 was XeO_3. Least-squares refinement of this model, utilizing a geometrically plausible XeO_3 group at site 2, yielded $R = 10.4\%$ for the Rb salt and $R = 11.0\%$ for the Cs salt using only those data not seriously affected by decomposition ($R = \Sigma\|F_o| - |F_c\|/\Sigma|F_o|$). In this and subsequent refinements, the following restrictions were placed on the occupancy factors of various sites (see Figure 1 and Table I for labeling of various atoms):

$$a_{Xe} + a_{Xe}* = 1.0$$

$$a_{M(0)} = a_{Cl(0)} \text{ (the "0.25 molecule" of MCl)}$$

$$a_{Cl(2)} = a_{O(1)} = a_{O(2)} = a_{O(3)} = a_{Xe} \text{ (the group at site 1)}$$

$$a_{Cl(2)*} = a_{O(1)*} = a_{O(2)*} = a_{O(3)*}$$
$$= a_{Xe*} \text{ (the group at site 2)}$$

With these restrictions, the site occupancies of the nondisordered atoms were sensibly close to that predicted by the $XeO_3\cdot2.25MCl$ stoichiometry.

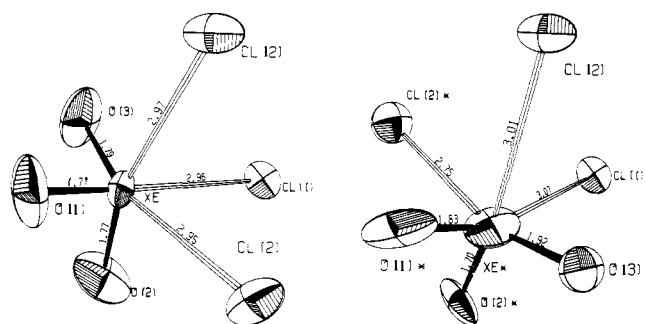At this point, fortunately, a crystal of the Cs salt weighing

Figure 1. The XeO_3Cl_3 units in $Cs_9(XeO_3Cl_2)_4Cl$. The left- and right-hand sides show the units occupying site 1 and site 2, respectively. The view is from approximately the $[1\bar{1}0]$ direction, with the z axis vertical.

approximately 3.5 mg was obtained. Although small by normal standards for neutron diffraction studies, a set of 795 reflections was collected, with no evidence of crystal damage, on the automated neutron diffractometer[6] at the Argonne CP-5 reactor. This included all reflections out to $2\theta = 90°$ (678 of which had intensity greater than 1σ) for $\lambda = 1.141$ Å. Lattice constants were determined to be $a = 16.587$ and $c = 7.087$ Å. Standard deviations for each reflection were calculated using the expression $\sigma^2(I) = TC + B + (0.02I)^2$, where I is net count, TC is total count, B is background, and 0.02 is an arbitrary coefficient. No absorption corrections were required because of the small crystal size. A neutron difference Fourier, using x-ray coordinates for the heavier atoms, clearly showed the existence of an XeO_3 group at site 2, as well as an associated chloride ion. The data refined to $wR = 8.3\%$ ($I > \sigma$), where wR

Table IV. Bond Distances and Angles around the Xenon Atoms

	Cs	Rb		Cs	Rb		Cs	Rb
Xe-O	1.77 (1)	1.78 (3)	O(1)-Xe-O(2)	101.2 (9)	105 (3)	O(1)-Xe-Cl(2)	88.4 (7)	91 (1)
Xe-O(2)	1.77 (2)	1.67 (8)	O(1)-Xe-O(3)	98.8 (10)	98 (3)	O(1)-Xe-Cl(1)	168.7 (5)	170 (1)
Xe-O(3)	1.78 (2)	1.55 (9)	O(2)-Xe-O(3)	101.6 (8)	98 (4)	O(1)-Xe-Cl(2)^a	84.8 (6)	87 (1)
Xe-Cl(2)	2.95 (2)	2.94 (1)	Cl(2)-Xe-Cl(1)	83.2 (3)	81.5 (5)	O(2)-Xe-Cl(2)	90.8 (7)	95 (3)
Xe-Cl(1)	2.96 (1)	2.93 (1)	Cl(2)-Xe-Cl(2)^a	74.1 (2)	72.5 (1)	O(2)-Xe-Cl(1)	86.4 (7)	83 (3)
Xe-Cl(2)^a	2.97 (1)	2.95 (2)	Cl(1)-Xe-Cl(2)^a	85.6(3)	84.4 (4)	O(2)-Xe-Cl(2)^a	163.7 (8)	163 (3)
						O(3)-Xe-Cl(2)	164.0 (8)	162 (3)
						O(3)-Xe-Cl(1)	87.5 (7)	88 (3)
						O(3)-Xe-Cl(2)^a	92.5 (8)	92 (3)
Xe*-O(1)*	1.83 (4)	1.78 (8)	O(1)*-Xe*-O(2)*	102 (3)	82 (4)	O(1)*-Xe*-Cl(2)*	85 (2)	93 (3)
Xe*-O(2)*	1.70 (6)	1.95 (11)	O(1)*-Xe*-O(3)*	87 (2)		O(1)*-Xe*-Cl(1)	162 (3)	172 (3)
Xe*-O(3)*	1.92 (7)		O(2)*-Xe*-O(3)*	115 (3)		O(1)*-Xe*-Cl(2)^a	83 (2)	98 (3)
Xe*-Cl(2)*	2.75 (5)	2.84 (8)	Cl(2)*-Xe*-Cl(1)	83 (1)	80 (2)	O(2)*-Xe*-Cl(2)*	90 (3)	76 (4)
Xe*-Cl(1)	3.07 (3)	2.95 (1)	Cl(2)*-Xe*-Cl(2)^a	77 (1)	77 (2)	O(2)*-Xe*-Cl(1)	89 (2)	92 (3)
Xe*-Cl(2)^a	3.01 (3)	2.90 (2)	Cl(1)-Xe*-Cl(2)^a	82 (1)	84 (1)	O(2)*-Xe*-Cl(2)*	165 (4)	153 (3)
						O(3)*-Xe*-Cl(2)*	153 (2)	
						O(3)*-Xe*-Cl(1)	105 (2)	
						O(3)*-Xe*-Cl(2)*	79 (2)	

^{a} Coordinates transformed by $\frac{1}{2} - x, \frac{1}{2} - y, -\frac{1}{2} + z$.

Table V. Bond Distances around the Metal Atoms ^{h}

	Cs	Rb		Cs	Rb
		M(1)-X Distances			
O(2)^b	3.47 (2)	3.01 (8)	O(2)*^{a}	3.49 (5)	3.63 (11)
O(3)^c	3.46 (2)	3.21 (8)	Cl(2)*^{c}	3.95 (4)	3.60 (8)
Cl(1)^a	3.52 (1)	3.44 (2)			
Cl(1)^c	3.53 (1)	3.37 (1)			
Cl(1)^d	3.57 (1)	3.34 (1)			
Cl(2)^a	3.57 (1)	3.42 (3)	O(3)*^{a}	3.94 (5)	
Cl(1)^a	3.60 (1)	3.44 (3)			
Cl(2)	3.78 (1)	3.78 (2)	O(3)*	3.41 (5)	
			O(1)*	3.37 (3)	3.58 (8)
		M(2)-X Distances			
O(2)^e	3.09 (2)	3.05 (8)	O(2)*^{e}	3.10 (5)	2.67 (11)
O(3)^f	3.17 (2)	3.08 (21)	Cl(2)*^{f}	3.16 (4)	2.98 (8)
Cl(0)	3.36 (1)	3.23 (1)			
O(1)^c	3.38 (2)	3.00 (4)	O(1)*^{c}	3.26 (4)	2.98 (8)
Cl(2)^a	3.39 (1)	3.20 (2)	O(3)*^{a}	3.55 (6)	
Cl(1)	3.44 (1)	3..31 (1)			
Cl(2)	3.53 (1)	3.52 (2)	O(3)*	3.43 (5)	
		M(0)-X Distances			
O(1)	3.04 (1)	2.80 (3)	O(1)*	3.63 (4)	3.42 (8)
Cl(0)^g	3.55 (1)	3.42 (1)	Cl(2)*	3.84 (4)	3.92 (8)

^{a} Coordinates transformed by $\frac{1}{2} - x, \frac{1}{2} - y, -\frac{1}{2} + z$. ^{b} Coordinates transformed by $-y, x, z$. ^{c} Coordinates transformed by $\frac{1}{2} - x, \frac{1}{2} - y, \frac{1}{2} + z$. ^{d} Coordinates transformed by $y, 1 - x, -z$. ^{e} Coordinates transformed by $\frac{1}{2} + y, \frac{1}{2} - x, \frac{1}{2} - z$. ^{f} Coordinates transformed by $\frac{1}{2} - y, \frac{1}{2} - x, -\frac{1}{2} - z$. ^{g} Coordinates transformed by $\frac{1}{2} - y, \frac{1}{2} + x, \frac{1}{2} - z$. ^{h} Columns 2 and 3 give the distances to the surrounding atoms excluding those atoms from site 2. Columns 5 and 6 give the new distances when an atom (or atoms) from a molecule in site 2 replaces an atom from a molecule in site 1.

$= \Sigma w(|F_o|^2 - |F_c|^2)/\Sigma w|F_o|^2$, with 80 (2)% occupancy of site 1. This relatively high R value reflects the large percentage of weak reflections due to the small sample size. The standard deviation of a reflection of unit weight was ~1.0 indicating the excellence of the overall fit. The final positional and thermal parameters for the Cs salt (based on the neutron diffraction data) and the Rb salt (based on the x-ray diffraction data) are given in Table I. Tables II and III list the observed and calculated structure factors for the Cs and Rb salts, respectively. Bond distances and angles are reported in Tables IV and V.

Computer programs used in performing these calculations, with their accession names in the "World List of Crystallographic Computer Programs", 3rd ed, are as follows: data reduction bond absorption correction, DATALIB; least-squares refinement, ORXFLS3; distances and angles, ORFFE3; structure drawings, ORTEP2.

Structure Description

The dominant feature of the structures is the interaction of each XeO_3 molecule with three chloride ions from the lattice to form a distorted octahedral XeO_3Cl_3 moiety. Bridging chloride ions tie these units together into $(XeO_3Cl_2)_n^{2n-}$ chains parallel to the c axis. For purposes of visualizing the structure, two other chains (not mutually exclusive from the first) can be identified in the remainder of the structure. One chain has stoichiometry $(MO_4 - ClCs_4)_{n/2}^{2n+}$ and the other has stoichiometry $(M_2Cl_2)_n$. The acentric nature and disorder present in the structure can be rationalized in terms of interactions between the two charged chains. The structure of the $(XeO_3Cl_2)_n^{2n-}$ chain and the nature of the disorder present will be discussed first. Then a description of the other two chains and the packing between the chains will be given. Except

where noted, the description refers to the structure of the Cs salt based on the neutron observations.

The disorder present in the structure has been taken into account in a physically realistic manner only for five pairs of atoms. These are Xe, O(1), O(2), O(3), and Cl(2), associated with the XeO_3Cl_3 unit at site 1, and Xe*, O(1)*, O(2)*, O(3)*, and Cl(2)*, associated with the XeO_3Cl_3 unit at site 2. The remainder of the atoms (Cs(O), Cs(1), Cs(2), Cl(0), and Cl(1)) may well also be disordered, but, if so, the disorder is too slight to be resolved by Fourier methods. Unusually large thermal motion is observed for these atoms along certain directions in the crystal. The positions reported for these five atoms then must represent mean or average locations, albeit dominated by the contribution from the "ordered" arrangement (i.e., occupancy of site 1). In the description of the structure, attention will be called to instances where it is thought that significant shifts for these atoms are caused by the disorder.

The XeO_3Cl_3 Units. The XeO_3Cl_3 units associated with sites 1 and 2 of the Cs salt are shown in Figure 1. It should be emphasized that the coordinates of the atoms associated with site 2 show serious systematic errors due to the near overlap of these atoms with atoms associated with site 1. Since the mean geometry of the species in site 2 is the same as that in site 1, the geometry observed for site 1 is felt to be the true representation of the XeO_3Cl_3 unit. It is this geometry which will be discussed in this section.

The pertinent features of this unit are illustrated in the left-hand side of Figure 1. The XeO_3Cl_3 unit has nearly ideal C_{3v} symmetry. Average bond distances and angles are Xe-O = 1.77 (2) Å, Xe-Cl = 2.96 (2) Å, O-Xe-O = 100 (1)°, Cl-Xe-Cl = 81 (6)°, O-Xe-Cl = 88 (3)°, and O-Xe-Cl = 166 (2)°. For comparison Xe-O distances and O-Xe-O angles are 1.76 (3) Å and 103 (4)° in XeO_3[7] and 1.77 (2) Å and 100 (2)° in $KXeO_3F$, where a five-coordinate XeO_3F_2 group exists.[4]

The unit at site 2, shown in the right-hand side of Figure 1, is significantly distorted from C_{3v} symmetry if the structure parameters are taken at face value. However, the deviations from C_{3v} observed in the XeO_3 moiety can be ascribed to refinement errors due to the near overlap of the disordered XeO_3Cl groups and we believe that the XeO_3 moieties have the same basic geometries at both sites. The Xe*-Cl(2)* distance is significantly shorter than the Xe-Cl distances at site 1, and is likely real.

The environment around each of the oxygen atoms at site 1 is very similar. In addition to the Xe-O bond at 1.77 Å, each oxygen atom interacts with one Cs ion at 3.05-3.17 Å and with a second Cs ion at 3.39-3.48 Å. More will be discussed about the significance of these interactions in a later section. The environment at site 2 is similar for O(2)* (Cs ions at 3.12 and 3.47 Å) and O(1)* (neighbors at 3.25 and 3.36 Å). However, since O(3)* is at approximately the same location as Cl(2), it has many interactions, including a Xe at 3.01 Å and four Cs at 3.16-3.55 Å. Thus, the disorder introduces no unusual contacts.

The $(XeO_3Cl_2)_n^{2n-}$ Chain. The structure of an idealized $(XeO_3Cl_2)_n^{2n-}$ chain, composed only of XeO_3Cl_3 units associated with site 1, is shown in the left-hand side of Figure 2. Each chain spirals around a 2_1 screw axis parallel to c which passes through $(x, y) = (\frac{1}{4}, \frac{1}{4})$, etc. The chain is characterized by nearly linear Xe-Cl-Xe bridges. This bridging angle is 168.0 (5)° in the Cs salt and 157.9 (8)° in the Rb salt. The smaller angle in the Rb salt is a direct consequence of the shorter length of the c axis. The two bridging Xe-Cl(2) distances in each salt are equal within 2σ. Surprisingly, the terminal Xe-Cl(1) bonds are the same length as the bridging bond lengths. However, it is seen that both types of chlorine atoms have six nearest neighbors. Thus, in the Cs salt, Cl(1)
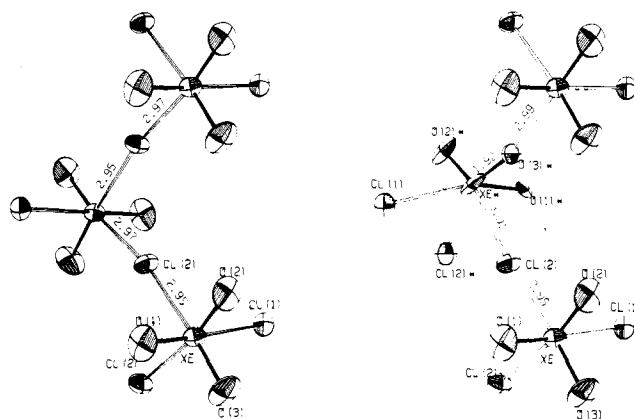

Figure 2. Illustration of the $(XeO_3Cl_2)_n^{2n-}$ chain. The left-hand side shows an idealized ordered arrangement composed of only site 1 units. The right side shows a typical disordered chain containing one site 2 unit. The orientation is the same as in Figure 1.

has one Xe at 2.96 Å and five Cs at 3.44, 3.52, 3.53, 3.57, and 3.60 Å, while Cl(2) has two Xe at 2.95 and 2.97 Å and four Cs at 3.39, 3.53, 3.57, and 3.78 Å. The coordination around Cl(2) is roughly octahedral, with two Xe (2.95 and 2.97), two Cs(1) (3.57 and 3.78 Å), and two Cs(2) (3.39 and 3.53 Å).

The chlorine bridging observed here can be compared with the fluorine bridging found in $KXeO_3F$[4] and in (Xe_2F_{11})-AuF_6.[8] In the former compound, the bridge is clearly asymmetrical (Xe-F = 2.36 and 2.48 Å) and very definitely nonlinear (Xe-F-Xe = 135°). In the latter case, the bridge is more nearly symmetrical (Xe-F = 2.21 and 2.26 Å) and close to being linear (Xe-F-Xe = 170°). It appears that the linearity of the bridge is a matter of steric effects and not an intrinsic characteristic of the halogen bridge.

The Disordered $(XeO_3Cl_2)_n^{2n-}$ Chain. The disordered $(XeO_3Cl_2)_n^{2n-}$ chain contains XeO_3Cl_3 groups which are rotated by 90° about a direction defined by a Cl(2)-O(2)* vector as shown on the right-hand side of Figure 2. This places O(3)* in the bridging position, giving an asymmetrical, yet nearly linear (167°), Xe-O-Xe bridge. It is significant that this rather unusual bridging arrangement can compete with the more conventional halide bridge. The Xe-O distance (2.99 Å) in the bridge is 0.2 Å longer than similar bridging distances which occur in XeO_2F_2[6] and XeO_3.[7] In the latter compounds, it it those bridges which make the largest contribution to the intermolecular forces in the crystalline lattice. Even at 2.99 Å, the long Xe-O distance is considerably shorter than the sum of the van der Waal radii (3.6 Å), so it is evident that this is a significant bonding interaction. Nevertheless, it certainly must be a weaker interaction than the corresponding Xe-Cl bridge, but this is compensated for by the formation of a very short Cl(2)*-Cs(2) bond. The nominal distance of 3.16 Å is unrealistically short, and it is likely that when site 2 is occupied, Cs(2) moves slightly in the z direction to give a more reasonable distance. This proposed disorder of Cs(2) was not detected directly, but accounts for the relatively large thermal motion in z direction for that atom (root mean square amplitude of vibration = 0.25 Å). The same effect is observed in the Rb salt (Rb(2)-Cl(2)* = 2.98 Å).

The $(CsO_4-ClCs_4)_{n/2}^{2n+}$ Chain. This chain, which involves the Cs and Cl atoms in special positions, is illustrated in Figure 3 for the idealized ordered structure. It runs parallel to the c axis, passing either through $(x, y) = (0, 0)$ or $(\frac{1}{2}, \frac{1}{2})$. The Cs(0)-Cl(0) distance in the chain is exactly half of the length of the c axis. It is this spacing, along with similar Cs-Cl interactions in the $(Cs_2Cl_2)_n$, which determines the c axis lattice constant. Both Cs(0) and Cl(0) are in near octahedral environments, but it must be emphasized that the structure illus-
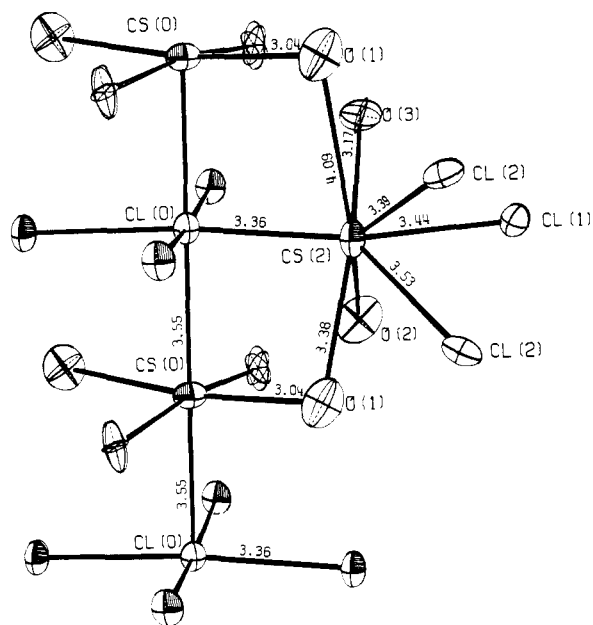
Figure 3. A view of the $(CsO_4-ClCs_4)_{1/2n}^{2n+}$ chain and of the coordination geometry around Cs(2) from approximately the [100] direction with the z axis vertical. Cs ellipsoids shown with octant shading, Cl ellipsoids with axes omitted, and O ellipsoids without enveloping ellipse.
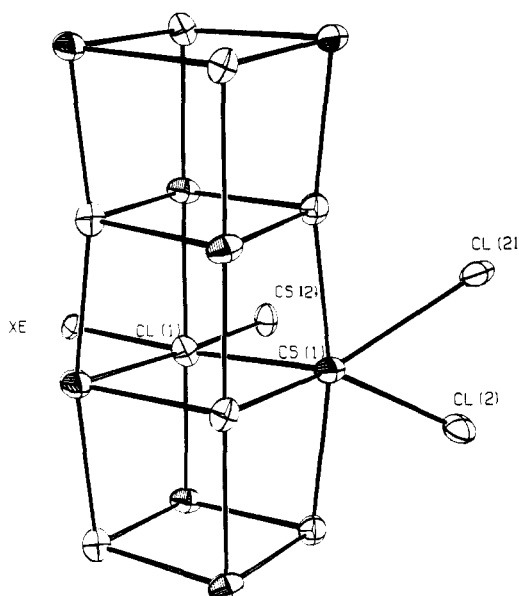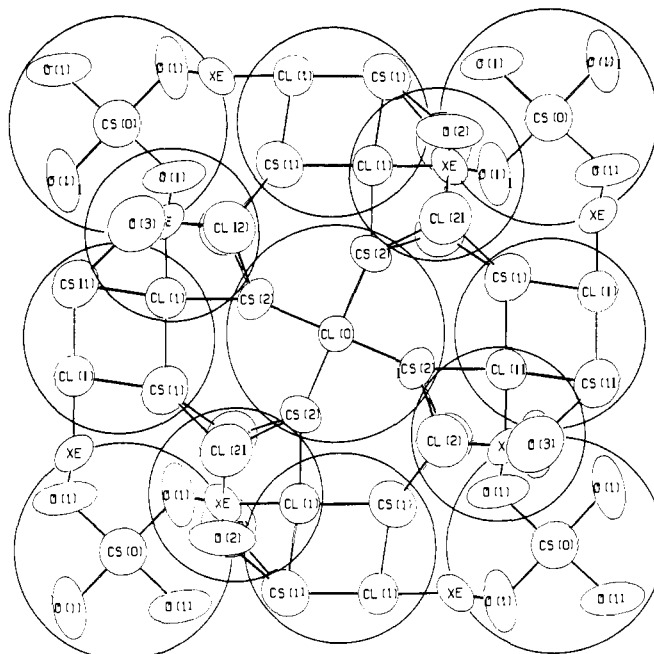

Figure 5. Projection onto the ab plane of the contents of the unit cell between $z = \frac{1}{4}$ and $z = -\frac{1}{4}$. The small circles identify the $(XeO_3Cl_2)_n^{2n-}$ chains, the medium-sized circles the $(Cs_2Cl_2)_n$ chains, and the large circles the $(CsO_4-ClCs_4)_{1/2n}^{2n+}$ chains.

Figure 4. A view of the $(Cs_2Cl_2)_n$ chain and of the coordination geometry around Cs(1) and Cl(1) from approximately the [210] direction with the z axis vertical. Atoms interior to the chain shown with ellipse axes (and octant shading for the Cs atoms) and atoms exterior to the chain shown without ellipse axes.

trated is for the idealized ordered situation, and the disorder will alter the coordination around Cs(0). This point will be discussed in fuller detail when the cause of the disorder is discussed. However, it should be noted at this point that a charge unbalance exists in the region of Cs(0). In the chain, the CsO_4 and $ClCs_4$ monomeric units are neither staggered nor eclipsed, but a gauche configuration is assumed with a dihedral angle of approximately 22°. Cs(2) assumes an irregular sevenfold coordination, illustrated in Figure 3, involving four chlorine and three oxygen atoms.

The $(Cs_2Cl_2)_n$ Chain. This chain, which stacks along the $\overline{4}$ axes which run parallel to the z axis through $(x, y) = (0, \frac{1}{2})$ and $(\frac{1}{2}, 0)$, is illustrated in Figure 4. This strictly ionic chain

contains only the Cs(1) and Cl(1) atoms, the latter also being a part of the $(XeO_3Cl_2)_n^{2n-}$ chains. Each Cs_2Cl_2 unit is nearly planar, and rhombic in shape (Cs(1)–Cl(1)–Cs(1) = 98.1° and Cl(1)–Cs(1)–Cl(1) = 81.8°). Adjacent units along the chain are related by the $\overline{4}$ operation and it is the Cs–Cl interaction along the chain which helps determine the c axis dimension. Cl(1) assumes a rough octahedral coordination with one Xe at 2.96 Å and 5 Cs at 3.51–3.60 Å. Cs(1) has a sixfold chloride ion coordination (6 Cl at 3.51–3.78 Å) which is not octahedral, the interaction with the Cl(2) atoms in the $(XeO_3Cl_2)_n^{2n-}$ chain precluding an octahedral configuration. There are two additional oxygen neighbors at a distance (~3.5 Å), somewhat longer than the normal metal–oxygen approach.

The Total Structure. The complete structure can now be mentally syntheiszed by fusing together the three types of chains discussed. This is illustrated in Figure 5, where the contents of the structure between $z = \frac{1}{4}$ and $z = -\frac{1}{4}$ are projected onto the ab plane. The smaller circles surrounding the Xe atoms represent the $(XeO_3Cl_2)_n^{2n-}$ chains, the medium-sized circles along the a and b axes represent the $(Cs_2Cl_2)_n$ chains, while the $(CsO_4-ClCs_4)_{n/2}^{2n+}$ chains are represented by the larger circles at the corners and face center. The bonds within a given chain are shown by heavy lines and the interactions (or bonds) between chains are shown by the lighter lines. First, it is noted that the $(XeO_3Cl_2)_n^{2n-}$ chains have Cl(1) atoms in common with the $(Cs_2Cl_2)_n$ chains and O(1) atoms in common with the $(CsO_4-ClCs_4)_{n/2}^{2n+}$ chains. In addition, the xenon chains are also tied to these latter two chains by Cs(1)–Cl(2) and Cs(2)–Cl(2) interactions, respectively. Finally, Cs(2)–Cl(1) interactions link these latter two chains together.

The Acentric Nature of the Structure. Examination of the crystal structure seems to indicate that it is the interaction of the XeO_3 molecule with the Cs(2) ions which causes the structure to be acentric. In the hypothetical centrosymmetric structure, a XeO_3 molecule would lie athwart the mirror plane at $z = 0$ as shown in Figure 6. Four Cs(2) atoms would lie around the XeO_3 molecule on the mirror planes at $z = \pm\frac{1}{2}$. The Cs(2)–O(2) and Cs(2)–O(3) distances would be a rea-
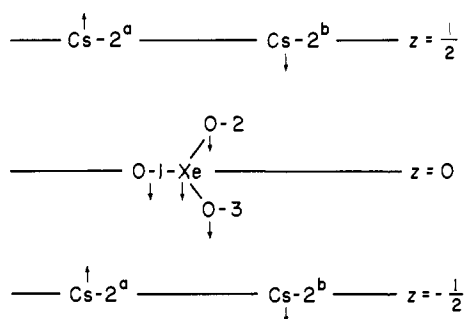
Figure 6. Diagram of the environment around the XeO_3 group in the hypothetical centrosymmetric structure. The arrows represent the direction of observed displacements in the acentric structure.

Figure 7. Illustration of the environment in the ab plane of Cs(0). The left-hand side shows the idealized ordered structure, the right-hand side a typical disordered arrangement. The view is from the [001] direction.

sonable length ($\sim$3.4 Å) but the Cs(2)–O(1) distances of $\sim$3.7 Å would be too long. This distance could be shortened by rotating the $ClCs_4$ grouping toward a more eclipsed configuration with respect to the CsO_4 grouping, but this would lengthen the Cs(2)–O(2) and Cs(2)–O(3) distances. However, by moving the XeO_3 group off the mirror plane (in the $-z$ direction as illustrated by the arrows in Figure 6), one of the Cs(2)–O(1) distances can be shortened. Concomitantly, that Cs (labeled Cs(2)[a] in Figure 6) can move up off its mirror plane to further shorten that Cs(2)–O(1) distance. The Cs atoms labeled Cs(2)[b] must now move down in order to retain reasonable distances to O(2) and O(3). Since Cs(2)[b] is related to Cs(2)[a] by a 90° rotation about the c axis, this defines a $\bar{4}$ rotation, rather than a simple fourfold rotation. Thus, the nonpolar space group $I\bar{4}$ is the space group in which the salts crystallize.

The Source of the Disorder. The cause of a disorder is often difficult to pinpoint, especially in a structure as complicated as this one is, where so many interactions are affected by the disorder. However, one feature stands out in examining the structure, and that is the interaction of the XeO_3Cl_3 units in sites 1 and 2 with the metal ion at the origin. In the "ordered" arrangement, four O(1) atoms coordinate to Cs(0) at a distance of 3.04 Å, as illustrated in the left-hand side of Figure 7. The octahedral coordination is completed by two Cl(0) at 3.54 Å (not shown in Figure 7). Although the oxygen atoms have a partial negative charge due to the nature of the Xe–O bond, it is doubtful that this is sufficient to offset the positive charge of the cesium ion. For comparison, the coordination sphere of Cs(1) has six chlorines (plus two oxygens at 3.5 Å) and of Cs(2) has four chlorines and three oxygens. Thus, the coordination around Cs(0) must result in inadequate charge compensation around that atom, at least in comparison to Cs(1) and Cs(2).

In order to alleviate this relative charge unbalance around Cs(0), it is postulated that one of the XeO_3Cl_3 groups at site 1 can be replaced by a group at site 2. The resulting configuration is illustrated by the right-hand side of Figure 7. This results in one of the Cs(0)–O(1) interactions being replaced by a Cs(0)–Cl(1)* and a long Cs(0)–O(1)* interaction (see Table V). The actual Cs(0)–Cl(2)* and Cs(0)–O(1)* distances may be shorter than the value listed in Table V since the cesium more than likely shifts off from the special position when site 2 is occupied. This is born out by its amplitude of thermal motion in the ab plane and by the residual scattering density around Cs(0). The latter shows that placing the cesium atom at the origin results in too much scattering density at the origin and some residual density unaccounted for in the ab plane.

The inclusion of the additional chlorine into the coordination sphere of Cs(0), with the concomitant replacement of chlorines
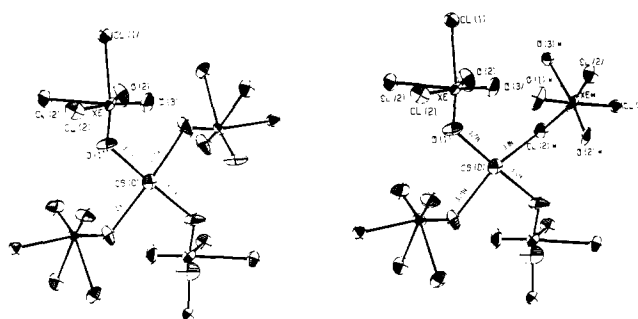
by oxygen in the other coordination sphere, reduces the relative charge imbalance. The observed occupancy of site 2 (20%) corresponds to four out of every five Cs(0) atoms having the configuration shown on the right-hand side of Figure 7 and one of five having the left-side configuration. For the Rb salt, 30% occupancy is observed, which corresponds to four of five having one site 2 group occupied and one of five having two site 2 groups occupied. The higher occupancy of site 2 in the Rb salt is rationalized by the smaller volume, and thus higher charge density, of the Rb^+ ion as compared to the Cs^+ ion. Another factor which may influence this is the short Cl(2)–Cl(2) contact of 3.43 Å in the Rb salt. This is a shorter than normal ionic contact (3.6 Å), but this contact distance is not uncommon when both chlorines are bonded to the same atom. Nevertheless, some strain could be removed by replacing one of these bridging chlorines with a O(3)* atom. The Cl(2)–Cl(2) distance is 3.57 Å in the Cs salt.

Conclusion

In conclusion, definite Xe–Cl bonds are shown to exist at room temperature. The observed Xe–Cl distance of 2.96 Å is markedly shorter than the van der Waals sum, 4.02 Å, for Xe and Cl. It is also lengthened by $\sim$0.66 Å with respect to an expected Xe–Cl single bond distance in good analogy with the $\sim$0.5 Å lengthening observed for Xe–F in $KXeO_3F$. The near equivalence of the terminal and bridging Xe–Cl separations, while surprising at first glance, may be attributed to rather similar coordination spheres about the two Cl atoms. The presence of the extra 0.25 mol of CsCl is probably required for lattice stabilization.

References and Notes

(1) Based on work performed under the auspices of the U.S. Atomic Energy Commission.
(2) G. J. Perlow and M. R. Perlow, *J. Chem. Phys.*, **48**, 955 (1968).
(3) P. LaBonville, J. R. Ferraro, and T. M. Spittler, *J. Chem. Phys.*, **55**, 631 (1971).
(4) D. J. Hodgson and J. A. Ibers, *Inorg. Chem.*, **8**, 326 (1969).
(5) E. R. Howell, D. C. Phillips, and D. Rogers, *Acta Crystallogr.*, **3**, 210 (1950).
(6) S. W. Peterson, R. D. Willett, and J. L. Huston, *J. Chem. Phys.*, **59**, 453 (1973).
(7) D. H. Templeton, A. Zalkin, J. D. Forester, and S. M. Williamson in "Noble Gas Compounds", H. H. Hyman, Ed. University of Chciago Press, Chicago, Ill., 1963, p 221.
(8) K. Leary, A. Zalkin, and N. Bartlett, *Inorg. Chem.*, **13**, 775 (1974).